View metadata, citation and similar papers at core.ac.uk

brought to you by CORE

provided by NASA Technical Reports Server

Subtropical Gyre Variability as seen from Satellites

SERGIO R. SIGNORINI[*,†] and CHARLES R. McCLAIN[*]

[*]NASA Goddard Space Flight Center

[†]Science Applications International Corp.

†Corresponding author. Email address: sergio.signorini@nasa.gov

Abstract:

A satellite multi-sensor approach is used to analyse the biological response of open ocean regions of the subtropical gyres to changes in physical forcing. Thirteen years (1998-2010) of SeaWiFS chlorophyll *a* (Chl-a), combined with concurrent satellite records of sea-surface temperature (SST) and sea level height, were analysed to investigate the seasonal and interannual variability of Chl-a concentration within these immense so-called ocean deserts. The seasonal variability of Chl-a within the gyres is driven mostly by the warming/cooling of surface waters. Summer warming promotes shallower mixed layers and lower Chl-a due to a reduction of vertical mixing and consequently a decrease in nutrient supply. The opposite happens during the winter cooling period. Therefore, long-term trends in SST have the potential to cause an impact on the interannual variability of Chl-a. Our analyses show that, during the 13 whole years of SeaWiFS data record, the North Pacific, Indian Ocean, and North Atlantic gyres experienced a decrease in Chl-a of 9%, 12%, and 11%, respectively, with corresponding SST increases of 0.27^{o}C, 0.42^{o}C, and 0.32^{o}C. The South Pacific and South Atlantic gyres also showed warming trends but with weak positive trends in Chl-a that are not statistically significant. We hypothesize that the warming of surface waters in these two gyres are counterbalanced by other interacting physical and biological driving mechanisms, as indicated in previous studies.

†Corresponding author. Email address: sergio.signorini@nasa.gov

1. Introduction

Subtropical gyre variability as seen from ocean colour satellites has been analysed in previous studies. *McClain et al.* (2004) showed that the oligotrophic waters of the North Pacific and North Atlantic gyres were observed to be expanding, while those of the South Pacific, South Atlantic, and South Indian Ocean gyres show much weaker and less consistent tendencies. Their results were based on 8 months (November 1996–June 1997) of Ocean-colour and Temperature Sensor (OCTS) and 6 years (September 1997–October 2003) of Sea-viewing Wide Field-of-View Sensor (SeaWiFS) ocean-colour data. *Polovina et al.* (2008) used a 9-year (1998-2006) time series of SeaWiFS to examine temporal trends in the oligotrophic areas of the subtropical gyres. They concluded that in the 9-year period, in the North and South Pacific, North and South Atlantic, outside the equatorial zone, the areas of low surface chlorophyll waters had expanded at average annual rates from 0.8 to 4.3%/yr. In addition, mean sea surface temperature in each of these 4 subtropical gyres also increased over the 9-year period, with the expansion of the low chlorophyll waters being consistent with global warming scenarios based on increased vertical stratification in the mid-latitudes.

Although the subtropical gyres are characterized by oligotrophic waters (low biomass and production), and quite often referred to as the ocean deserts, their immense size (they occupy ~40% of the surface of the earth) makes their contribution to the global carbon cycle very important. The upper kilometer of the subtropical gyres is primarily wind driven (Huang and Russell 1994). The horizontal and vertical motion in this layer plays a significant role in controlling the interaction between the atmosphere and ocean, which is of vital importance to our understanding of the oceanic general circulation and climate (Huang and Qiu 1994). The gyres are characterized by a deep pycnocline at their centers and strong horizontal gradients of temperature and salinity at the fringes due to pycnocline outcropping. The flow in the western limbs (western boundary currents) is intensified by the latitudinal changes of the Coriolis acceleration (β effect), while the flow is relatively weak in the gyres' eastern parts. The broad region of relatively weak flow occupies most of the gyre and is called the Sverdrup regime (Pedlosky 1990). The dynamic center of the gyres can be identified by a maximum sea-surface height (SSH). The pycnocline shoals in the mid-latitudes, where isopycnals outcrop at the Subtropical Front, and at the equator, where Ekman flow divergence promotes upwelling.

An important biological characteristic of the subtropical gyres is the large variability in phytoplankton growth rates with minimal changes in biomass (Laws et al. 1987, Marra and Heinemann 1987, Marañón et al. 2000, Marañón et al. 2003). Therefore, understanding the interactions between physical and biological processes within the subtropical gyres is central for determining the magnitude and variability of the carbon exported from the surface to the deep ocean.

We used a satellite multi-sensor approach to analyse the biological response of all five subtropical gyres to changes in physical forcing. A major data source for our analysis was the chlorophyll (Chl-a) data from the Sea-viewing Wide Field-of-view-Sensor (SeaWiFS), which has provided 13-years of continuous high-quality global data until recently (February 2011) when it stopped communicating with ground-based telemetry stations after months of intense efforts at recovery. Satellite-based sea-surface temperature (SST) were obtained from Optimally Interpolated (OI) AVHRR data (Reynolds et al. 2007) and dynamic height (*h*) from altimetry data. The results reported in this paper are based on data records that are longer than the ones used in similar previous efforts (McClain et al. 2004, Polovina et al. 2008). Both reported

†Corresponding author. Email address: sergio.signorini@nasa.gov

significant changes in the sizes of most gyres. The seasonal cycle and long-term trends of the physical forcing and biological response are analysed within the geographical domain of the subtropical gyres, based on the most recent reprocessing of the entire SeaWiFS data record, the only such record of adequate data quality for this analysis.

2. Methodology and Data Sources

The study domains for all five gyres, the North and South Pacific (NPAC and SPAC), the North and South Atlantic (NATL and SATL), and the South Indian Ocean (IOCE) gyres are shown in Fig. 1. The choice for the gyre domain polygons shown in Fig. 1 follows the methodology of *McClain et al.* (2004) with a few revisions. The oligotrophic regions (purple areas in Fig. 1) expand during summer and contract during winter following the seasonal strength of the winds and convective upper-ocean mixing. The rationale for choosing the size and shape of the study polygons is twofold: (1) they should contain the entire oligotrophic regions of the gyres during the maximum expansion in summer; and, (2) they should avoid peripheral regions where other dynamic processes prevail, such as coastal and equatorial upwelling, river discharge, and western and eastern boundary current systems.

Our analysis is based on three satellite data sources, 9-km monthly Chl-a from the latest SeaWiFS reprocessing (http://oceancolor.gsfc.nasa.gov/), 0.25^o daily SST (NOAA_OI_SST_V2 data provided by the NOAA/OAR/ESRL PSD, Boulder, Colorado, USA, from their Web site at http://www.esrl.noaa.gov/psd/), and 0.3^o weekly *h* from the multi-sensor altimeter data. Altimeter data used were produced by Ssalto/Duacs system and distributed by Aviso, with support from the Centre National d'Études Spatiales (CNES). All three satellite data products cover the common period of 1998-2010. The SST and *h* products were averaged to monthly values after the daily (SST) and weekly (h) time series of gyre domain averages were computed. Seasonal climatology and time series of averaged Chl-a, SST, and *h* were produced within the limit domains of all five gyres. The anomalies of each parameter were then calculated by removing the seasonal climatology from the time series and long-term trends derived for each parameter and gyre domain.

3. Discussion and Results

The seasonal cycles of Chl-a, SST, and *h* for the five gyres are shown in Fig. 2. The seasonal physical forcing and biological response within the five gyres are readily seen from the relative phasing of the annual cycles. The seasonality of *h* within the gyre indicates a contraction in winter and an expansion in summer, in phase with the size variability of the oligotrophic region inside the gyre. The common forcing factor in the Chl-a, *h*, and vertical mixing variability within the gyre is the seasonal change in surface thermal forcing (Signorini and McClain 2007). The warming of surface waters promotes shallower mixed layers, higher *h* resulting from elevated sea level height, and lower Chl-a due to reduced vertical mixing. The opposite happens during the winter cooling period. The higher *h* during summer indicates a strengthening of the gyre circulation and consequently promotes deeper thermocline/nutricline depths, which, combined with the shallower mixed layers, contributes to a reduction in the upward vertical transport of nutrients to the euphotic zone. Therefore, environmental changes, such as climate driven long-term warming trends in the surface ocean will drive a decline in nutrient renewal and, consequently, a reduction in phytoplankton biomass and productivity. However, other important competing physical processes contribute to the supply of nutrients to the interior of the

†Corresponding author. Email address: sergio.signorini@nasa.gov

gyres that help maintain phytoplankton productivity, such as the lateral nutrient transfer via Ekman horizontal transport at the gyre flanks (Williams and Follows 1998).

Fig. 3 shows the time series of Chl-*a*, SST, and *h* anomalies for all five gyres, and Table 1 summarizes their corresponding trends. All five gyres show warming trends and consistent positive *h* trends with SST. The largest trends occurred in the Indian Ocean with a Chl-a trend of -7.42×10^{-4} mg m^{-3} yr^{-1}, SST of +0.032 ^{o}C yr^{-1}, and *h* of +0.57 cm yr^{-1}. The signs of these trends in the Indian Ocean, and those of the North Pacific and North Atlantic gyres, are consistent with the expected forcing versus response as described above. Trends in the North Pacific gyre are -4.98×10^{-4} mg m^{-3} yr^{-1} for Chl-a, +0.020 ^{o}C yr^{-1} for SST, and +0.21 cm yr^{-1} for *h*, while in the North Atlantic the trends are -6.71×10^{-4} mg m^{-3} yr^{-1}, +0.025 ^{o}C yr^{-1}, and +0.097 cm yr^{-1}, respectively. The trend behavior for the South Pacific gyre is positive for Chl-a ($+1.16\times10^{-4}$ mg m^{-3} yr^{-1}) with corresponding positive trends for SST and *h* (+0.024 ^{o}C yr^{-1} and +0.32 cm yr^{-1}, respectively). Despite the relatively strong positive trends in SST (+0.027 ^{o}C yr^{-1}) and *h* (+0.29 cm yr^{-1}) in the South Atlantic gyre, the corresponding Chl-a trend ($+1.01\times10^{-4}$ mg m^{-3} yr^{-1}) is positive as well. However, the trends in these two gyres are significantly smaller than in the other gyres and have low statistical significance (see Table 1). This seems to indicate that the effect of the warming trend in surface waters and deepening of the thermocline/nutricline in the South Pacific and South Atlantic gyres are counterbalanced by other physical and/or physiological processes influencing the long-term variability of phytoplankton biomass, e. g., iron limitation (Behrenfeld et al. 2009), in which case decreases in macronutrients would have little effect.

The Indian Ocean gyre showed the largest warming trend (0.032^{o}C yr^{-1}). During the 13 years of SeaWiFS observations, the Indian Ocean gyre had an average SST increase of 0.42^{o}C with a corresponding decrease in Chl-a of 0.0096 mg m^{-3}, which translates into a Chl-a reduction of nearly 12% from the mean annual value of 0.081 mg m^{-3} in 1998. For the same time period, an SST warming of 0.32 ^{o}C in the North Atlantic gyre resulted in a Chl-a decrease of 0.009 mg m^{-3}, or a reduction 11% from the mean 1998 value of 0.081 mg m^{-3}. An equivalent assessment for the North Pacific gyre indicates a 13-year SST increase of 0.27^{o}C with a corresponding Chl-a reduction of 0.0065 mg m^{-3}, or 9.3% from the 1998 annual mean of 0.070 mg m^{-3}.

Vantrepotte and Mélin (2011) analysed the interannual variations in the SeaWiFS global Chl-a concentration for the period of 1997-2007. They identified open ocean regions presenting significant long-term monotonic changes in Chl-a over the SeaWiFS period. Their results showed strong negative Chl-a trends in most of the subtropical gyre areas, namely the tropical North Atlantic, the southwestern part of the South Atlantic gyre, the southeast Indian Ocean, a large part of the northern tropical Pacific as well as the South Pacific gyre. The 10 year data set shows a significant increase in Chl-a in a large region located in the northern part of the South Atlantic gyre that contrasts with the decrease found southwest of this oceanic domain, as well as significant positive trends in Chl-a in a large region of the southeastern South Pacific gyre (Vantrepotte and Melin 2009, Vantrepotte and Mélin 2011). This spatial variability in the sign of the trends explain our gyre-averaged findings, which showed weak, and statistically insignificant, positive trends in the South Pacific and South Atlantic gyres, while the other three gyres showed significant negative trends in Chl-a.

4. Summary and Conclusions

Analysis of 13 years (1998-2010) of concurrent multi-sensor satellite data (Chl-a, SST, and *h*) indicates that all five subtropical gyres are getting warmer with a corresponding increase

†Corresponding author. Email address: sergio.signorini@nasa.gov

in sea-surface elevation. Three of the gyres, the North Pacific, Indian Ocean, and North Atlantic, exhibit downward trends in Chl-a that are consistent with the increase in vertical stratification as a result of the observed warming trends. During the 13 whole years of SeaWiFS data record, these three gyres experienced a decrease in Chl-a of 9%, 12%, and 11%, respectively, with corresponding SST increases of 0.27^{o}C, 0.42^{o}C, and 0.32^{o}C. Previous studies (Vantrepotte and Melin 2009, Henson et al. 2010, Vantrepotte and Mélin 2011) have shown large coherent regions with Chl-a trends of opposite signs in both South Pacific and South Atlantic gyres. This is probably due to the intrusion of colder, nutrient-rich, waters from the Southern Ocean on the easternmost regions of these gyres, and the likely reason for the observed increase in Chl-a concentration counterbalancing downward trends in the subequatorial regions of the gyres.

The analyses presented here are intended to simply highlight the possible connections between biological and physical variability in the subtropical gyres on seasonal and interannual time scales. Although the present study is based on more expanded ocean colour records than previously achieved, much longer records will be required to establish robust correlation between the long-term variability of the subtropical gyres and climate trends. In fact, previous studies based on numerical model simulations suggest that up to 40 years of data records are required to identify climate effects (e.g., Henson et al. 2010). The exact nature of the couplings will require modeling studies in addition to the collection and analysis of longer satellite and in situ data records. Thus, it is important to emphasize that the 13-year observed trends here could be the signature of natural oscillations of frequency not entirely resolved by the relatively short record when compared to much longer time scales attributed to global climate change. Finally, these analyses are possible because of the unprecedented stability of the SeaWiFS time series, which is due to the use of monthly lunar calibrations and totally independent from the Earth-viewing data, a capability critical to future missions. It is not clear at this time that a longer time series using multiple satellite ocean colour data sets will allow further analyses like those presented here.

†Corresponding author. Email address: sergio.signorini@nasa.gov

Acknowledgements

We want to acknowledge the NASA Ocean Biology and Biogeochemistry Program for supporting this work.

†Corresponding author. Email address: sergio.signorini@nasa.gov

References

BEHRENFELD, M. J., WESTBERRY, T. K., BOSS, E. S., O'MALLEY, R. T., SIEGEL, D. A., WIGGERT, J. D., FRANZ, B. A., MCCLAIN, C. R., FELDMAN, G. C., DONEY, S. C., MOORE, J. K., DALL'OLMO, G., MILLIGAN, A. J., LIMA, I., and MAHOWALD, N., 2009, Satellite-detected fluorescence reveals global physiology of ocean phytoplankton. Biogeosciences, 6, 779-794.

HENSON, S. A., SARMIENTO, J. L., DUNNE, J. P., BOPP, L., LIMA, I., DONEY, S. C., JOHN, J., and BEAULIEU, C., 2010, Detection of anthropogenic climate change in satellite records of ocean chlorophyll and productivity. Biogeosciences, 7, 621-640.

HUANG, R. X., and QIU, B., 1994, Three-Dimensional Structure of the Wind-Driven Circulation in the Subtropical North Pacific. Journal of Physical Oceanography, 24, 1608-1622.

HUANG, R. X., and RUSSELL, S., 1994, Ventilation of the Subtropical North Pacific. Journal of Physical Oceanography, 24, 2589-2605.

LAWS, E. A., DITULLIO, G. R., and REDALJE, D. G., 1987, High Phytoplankton Growth and Production-Rates in the North Pacific Subtropical Gyre. Limnology and Oceanography, 32, 905-918.

MARAÑÓN, E., BEHRENFELD, M. J., GONZALEZ, N., MOURINO, B., and ZUBKOV, M. V., 2003, High variability of primary production in oligotrophic waters of the Atlantic Ocean: uncoupling from phytoplankton biomass and size structure. Marine Ecology-Progress Series, 257, 1-11.

MARAÑÓN, E., HOLLIGAN, P. M., VARELA, M., MOURINO, B., and BALE, A. J., 2000, Basin-scale variability of phytoplankton biomass, production and growth in the Atlantic Ocean. Deep-Sea Research Part I-Oceanographic Research Papers, 47, 825-857.

MARRA, J., and HEINEMANN, K. R., 1987, Primary Production in the North Pacific Central Gyre - Some New Measurements Based on C-14. Deep-Sea Research Part a-Oceanographic Research Papers, 34, 1821-1829.

MCCLAIN, C. R., SIGNORINI, S. R., and CHRISTIAN, J. R., 2004, Subtropical gyre variability observed by ocean color. Deep-Sea Res. Part II, 51, 281-301.

PEDLOSKY, J., 1990, The Dynamics of the Oceanic Subtropical Gyres. Science, 248, 316-322.

POLOVINA, J. J., HOWELL, E. A., and ABECASSIS, M., 2008, Ocean's least productive waters are expanding. Geophysical Research Letters, 35.

REYNOLDS, R. W., SMITH, T. M., LIU, C., CHELTON, D. B., CASEY, K. S., and SCHLAX, M. G., 2007, Daily high-resolution-blended analyses for sea surface temperature. Journal of Climate, 20, 5473-5496.

SIGNORINI, S. R., and MCCLAIN, C. R., 2007, Large-scale forcing impact on biomass variability in the South Atlantic Bight. Geophysical Research Letters, 34.

VANTREPOTTE, V., and MELIN, F., 2009, Temporal variability of 10-year global SeaWiFS time-series of phytoplankton chlorophyll a concentration. Ices Journal of Marine Science, 66, 1547-1556.

VANTREPOTTE, V., and MÉLIN, F., 2011, Inter-annual variations in the SeaWiFS global chlorophyll a concentration (1997-2007). Deep-Sea Research Part I-Oceanographic Research Papers, 58, 429-441.

WILLIAMS, R. G., and FOLLOWS, M. J., 1998, The Ekman transfer of nutrients and maintenance of new production over the North Atlantic. Deep-Sea Research Part I-Oceanographic Research Papers, 45, 461-489.

†Corresponding author. Email address: sergio.signorini@nasa.gov

Table 1. Linear trends of chlorophyll (*Chl**), sea-surface temperature (SST*), and Aviso dynamic height (*h**) anomalies for all five gyres. Domain regions are defined by the white polygons in Fig. 1. Units of linear slopes are mg m^{-3} yr^{-1} for *Chl**, ^{o}C yr^{-1} for SST*, and cm yr^{-1} *h**. The *p* value for the 95% confidence level was calculated for each regression. Values less than 0.05 are statistically significant. Except for values in bold, derived trends have *p* values much smaller than 0.05 and therefore statistically significant.

Gyre	*Chl**	SST*	*h**
NPAC	-4.9752e-4	+0.0204	+0.2127
SPAC	**+1.1567e-4**	+0.0236	+0.3218
IOCE	-7.4169e-4	+0.0322	+0.5712
NATL	-6.7140e-4	+0.0248	+0.0965
SATL	**+1.0116e-4**	+0.0266	+0.2845

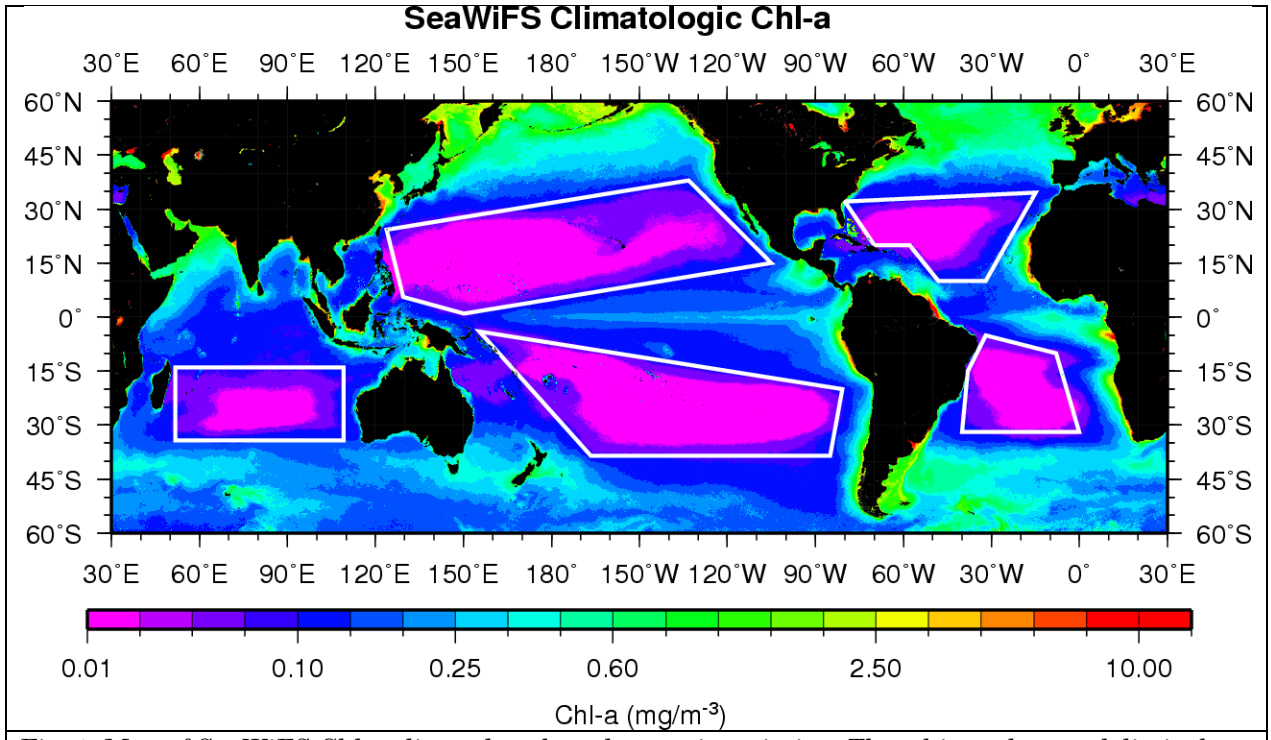

Fig. 1. Map of SeaWiFS Chl-a climatology based on entire mission. The white polygons delimit the analysis regions.

†Corresponding author. Email address: sergio.signorini@nasa.gov

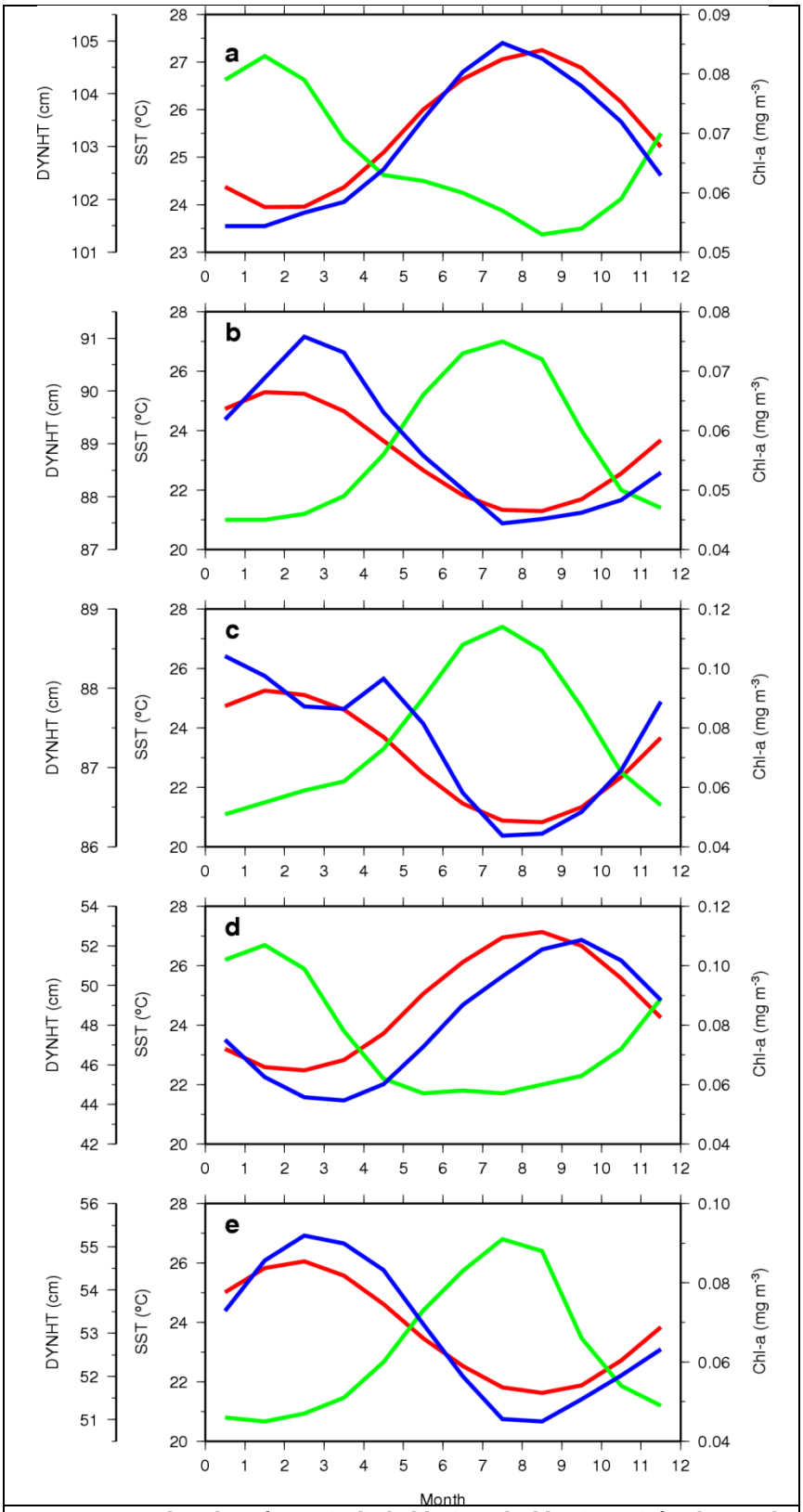

Fig. 2. Seasonal cycles of SST (red), *h* (blue), and Chl-a (green) for the North Pacific (a), South Pacific (b), Indian Ocean (c), North Atlantic (d), and South Atlantic (e) gyres.

†Corresponding author. Email address: sergio.signorini@nasa.gov

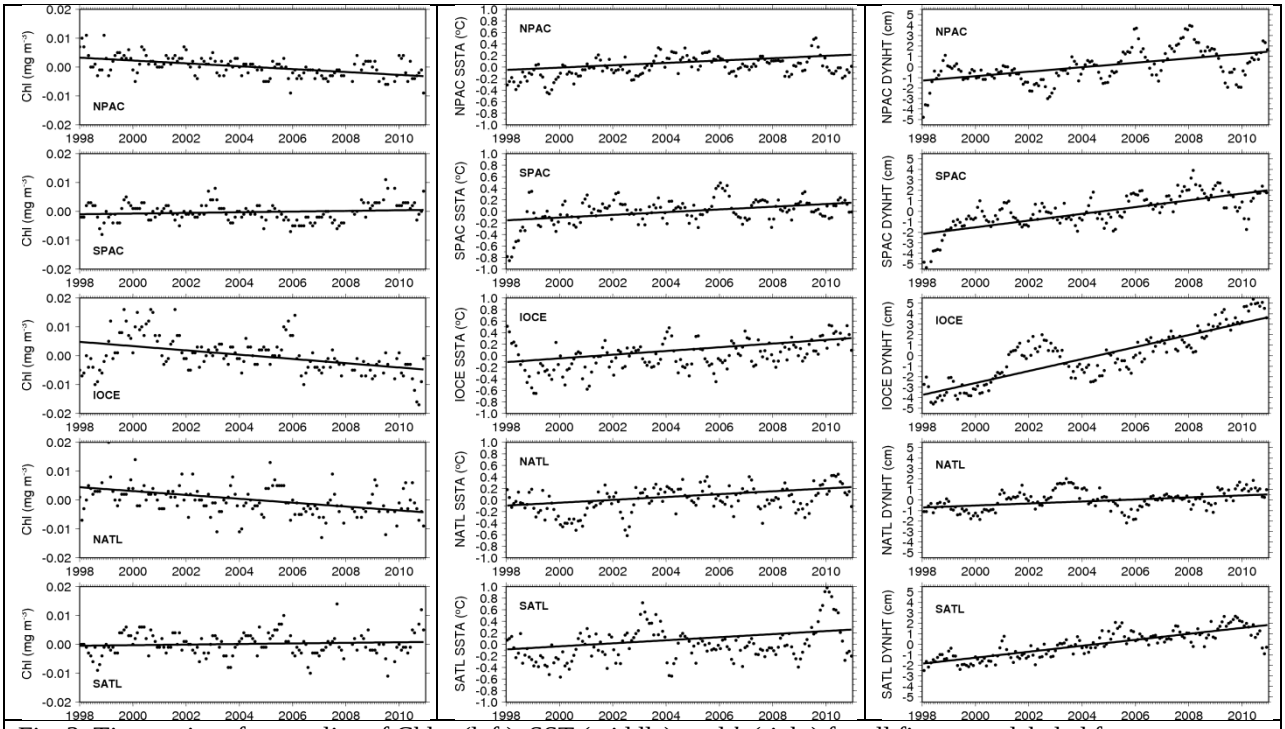

Fig. 3. Time series of anomalies of Chl-a (left), SST (middle), and *h* (right) for all five gyres labeled from top to bottom NPAC, SPAC, IOCE, NATL, and SATL. Corresponding trends are superposed.

†Corresponding author. Email address: sergio.signorini@nasa.gov